Application of Acoustic-solid Coupling Theory in New Energy Vehicle Noise Control

FUJUN MAO
Lyceum of the Philippines University,
Manila 1002,
PHILIPPINES

Abstract: - The development of new energy vehicles has attracted much attention due to the strong promotion and popularisation of the concept of low carbon and environmental protection, and the increasing demand for environmental protection in cars. Although these vehicles meet people's requirements for resource and environmental protection, the noise generated during the driving process affects the comfort of the vehicle occupants and the concentration of the vehicle driver. To address this problem, the research proposes to improve the noise control technology of new energy vehicles based on acoustic-solid coupling theory and to test the practical application effect of this technology. The test results show that the maximum acceleration of vibration at the roof, floor, axle head, and spring of the new energy vehicle are 1.48 m/s2, 1.02 m/s2, 0.079 m/s2, and 0.020 m/s2 respectively, which are lower than the maximum acceleration before the use of this technology. The maximum sound pressure at the windscreen and side window glass of the new energy vehicle is 80 dB(A) and 73 dB(A) after the use of this technology. The maximum sound pressure at the driver's ear was 62 dB(A) and 77 dB(A) when the vehicle was driven on different road surfaces, which were lower than the sound pressure values before use. In summary, the research proposes to improve the noise control technology of new energy vehicles based on the sound-solid coupling theory, which can have the effect of reducing the noise value generated by new energy vehicles and improving the comfort of users.

Key-Words: - New energy vehicles; Acoustic-solid coupling; Automotive noise; Noise control technology

1 Introduction

With the continuous development of science and technology, many new technologies are being used in many fields, and the automotive industry is developing very fast thanks to these technologies, [1]. With the gradual strengthening of the performance of cars, people's requirements for cars are no longer limited to their safety, [2], [3]. At the same time, the growing popularity of environmental protection theory has influenced people's demand for environmentally friendly cars. Based on this development trend, the automotive industry has developed new energy vehicles that do not use traditional fossil energy and reduce the consumption of non-renewable energy sources, which are very popular among people, [4], [5]. However, these vehicles generate a lot of noise during the driving process, which not only affects the comfort of the occupants and the driver's concentration but also produces noise pollution to the surrounding environment. To address this problem, the study proposes the use of acoustic-solid coupling theory to optimize the noise control technology of new energy vehicles. It is expected that this method will

effectively control the noise during the driving process of new energy vehicles and reduce the negative impact of noise. The innovation of this study is to use the acoustic-solid coupling theory, combined with the structural modal analysis of the new energy vehicle, to construct an acoustic-solid coupling system model to accurately monitor the noise inside the vehicle. The contribution of this study is that through in-depth research and exploration of the application of sound-structure coupling theory in the noise control of new energy vehicles, it provides a new idea and method for theoretical research in the field of noise control of new energy vehicles. By studying the noise sources of new energy vehicles, targeted noise control measures are proposed to reduce the internal noise of new energy vehicles, improve the riding comfort, improve the riding environment, improve the comfort and satisfaction of drivers and passengers, promote the promotion and popularization of new energy vehicles, and make contributions to environmentally friendly transportation. The first part of this study is a brief introduction to recent research on automotive noise and the application of

coupling theory. The second part presents a detailed study of the structure of new energy vehicles based on modal analysis, and the use of acoustic-solid coupling to optimize noise control techniques for new energy vehicles. The third part is an analysis of the practical application of the optimization methods proposed in the study of vehicle noise control technology. The final section summarises and analyses the research content.

2   Literature Review

With the increasing demand for comfort during the driving process, many scholars have been gradually deepening their research on automotive noise. Kim and Cho proposed a potential semantic control generative adversarial network method to address the problem that it is difficult to accurately classify noise types in automotive quality assessment. After comparative experimental analysis, the results show that the method has an accuracy of 96.68% in classifying noise data, and an accuracy of 94.68% for the interference case, [6]. Yu's team proposes a discrete wavelet-based noise suppression method for automotive driveline noise to address the problem of low efficiency of traditional methods of automotive driveline noise suppression, [7]. [8], proposed a fan blade with a ridged surface based on the bionic principle to replace the conventional fan blade and found that the sound pressure level of the fan blade was reduced by 3.83 dB(A) compared with the original blade after experimental analysis. [9], proposed a method for solving the acoustic perturbation equation based on incompressible separated vortex simulations of convective pressure pulsations, and after experiments, the results showed that the method could accurately calculate the sound pressure pulsations in the vehicle side windows, and thus calculate the noise generated to the interior of the vehicle. [10], proposed an improved denoise method based on EEMD and optimal wavelet threshold for model building of OPAX. The results show that the noise reduction effect of this method is better than that of the traditional method, which can better improve the accuracy of the road dynamics analysis model.

After more than a decade of development, coupled solutions have now become a popular research topic. [11], proposed a sequential iterative fluid-solid coupling scheme for thermal analysis to address the problem of low accuracy in loss calculation and temperature rise prediction in high-speed high-power switched reluctance motors, and after empirical analysis, the results show that the

scheme is faster and more accurate than the traditional one. Hou's team proposed a fluid-solid coupling-based finite element software modal analysis method for satellite flexo. The results show that the method can reduce the inherent frequency of the central impression cylinder and is feasible, [12]. Li's team proposed a method for the dynamic tracking of multiphase vortex flow and unclear critical vibration wave conversion using coupled. After comparative tests, the results show that the method can accurately calculate the nonlinear shock components concentrated in the frequency range of 45-50 Hz, [13]. Franci addressed the problem of incompressible tracking of fluids in fluid-structure interactions. A fully Lagrangian finite element method combining fluid-structure coupling with nodal integration is proposed, and after empirical analysis, the results show that the method has higher accuracy and better convergence than traditional methods, [14].

In summary, many scholars have used many high technologies to study automotive noise in recent years, and coupling theory has also been applied to several fields, but the number of scholars who have combined these two studies is still small. This study proposes to apply the acoustic-solid coupling theory to the noise control of new energy vehicles, hoping to fill the gap in this research direction through this method and provide a new idea for the subsequent vehicle noise reduction research.

3 Research on Noise Control Technology of New Energy Vehicles Based on Acoustic-solid Coupling Theory

With the continuous development of automotive technology and the popularity of the theory of sustainable development of resources, new energy vehicles have gradually integrated into people's lives. However, when using new energy vehicles, the noise inside the vehicle is high, which has an impact on the comfort of the driver as well as the occupants. Therefore, this chapter of the study proposes to optimize the noise control technology of new energy vehicles by using the sound-solid coupling theory.

3.1   Research on Structural Noise of New Energy Vehicles based on Modal Analysis Theory

The noise generated during the driving process of new energy vehicles will not only reduce the comfort of the car ride and affect the

communication of the vehicle occupants but will also reduce the driver's ability to cope with various emergencies to a certain extent, thus reducing the safety of the vehicle. There are various reasons for the production of noise in the vehicle, and the specific production mechanism is shown in Figure 1, [15].

As can be seen from Figure 1, the transmission of noise within a new energy vehicle can be divided into, according to the different transmission media, airborne sound transmission and solid sound transmission. Airborne sound transmission refers to the medium to high-frequency noise transmitted by the air cavity inside the vehicle, such as tire noise, engine vibration noise, etc. Solid sound transmission refers to the low-frequency noise generated by the body wall panels under the action of external excitation, such as road excitation, engine excitation, etc. resulting in noise generated by body vibration, etc., [16], [17]. Noise in the car can be divided into three categories according to the nature of the sound waves, namely structural noise, air noise, and cavity resonance, as shown in Figure 2.
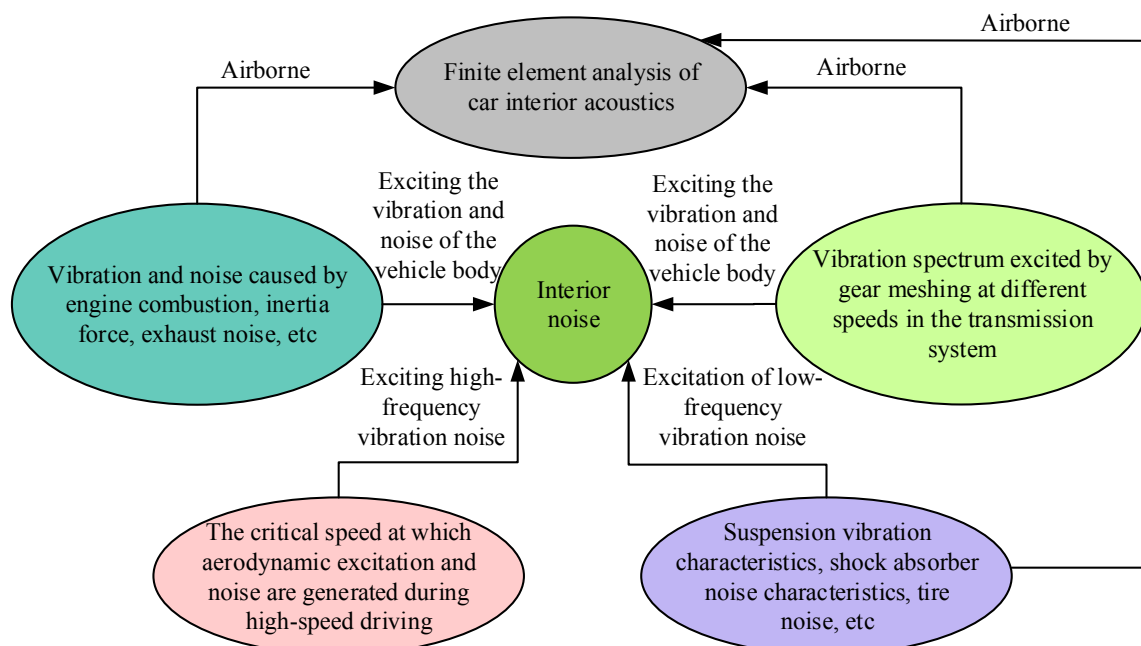
Fig. 1: Mechanism of noise generation in motor vehicles
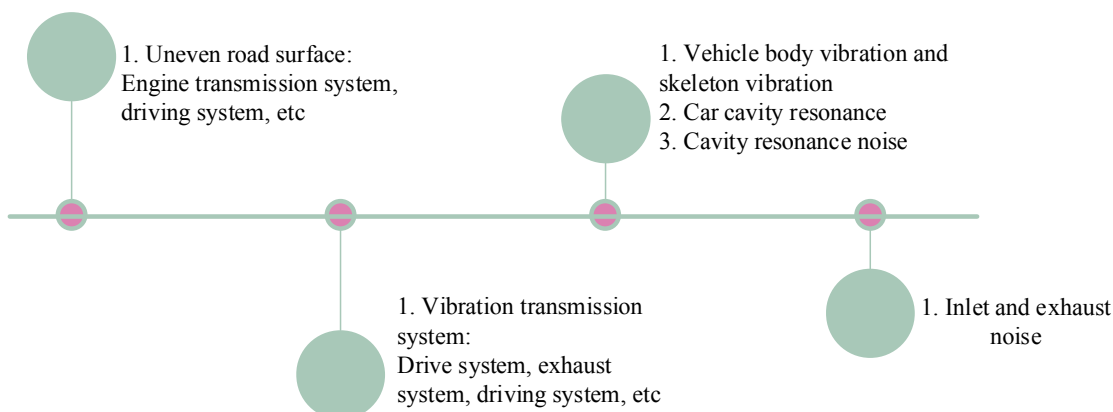
Fig. 2: In-vehicle noise classification

As can be seen from Figure 2, structural noise is noise radiated to the vehicle occupants by forced vibrations of the body wall panel structure. Air noise is generated because the sound of the outside air is transmitted through the vehicle gaps to the interior cavity when the vehicle is traveling at high speed. Cavity resonance noise is due to the fact that the noise is constantly reflecting itself as it is transmitted inside the vehicle, partially canceling and partially superimposing. Modal analysis techniques are a method of analysis based on vibration theory and aimed at modal parameters, [18]. The method can be used to understand the inherent vibration characteristics of a structure, to analyze complex structures, and to diagnose faults in components. It is therefore proposed to use this method to analyze the structure of a new energy vehicle and to provide a basis for predicting and controlling noise in the vehicle. Structural modal analysis uses the idea of the finite element method to transform the actual continuous, infinite degree of freedom structural vibration response problem of an object into a discrete, finite degree of freedom vibration problem, where the differential equations of motion for a multi-degree of freedom system are shown in Equation (1), [19].

shown in Equation (1), [19].

$$\{F(t)\} = [M]\{\ddot{X}\} + [C]\{\dot{X}\} + [K]\{X\} \tag{1}$$

Equation (1), $[M]$ represents the total mass matrix of the vehicle structure; $[C]$ represents the total damping matrix of the vehicle structure; $[K]$ represents the total stiffness matrix of the vehicle structure; $\{F(t)\}$ represents the external load vector of the vehicle; $\{\ddot{X}\}$ represents the acceleration of the vehicle; $\{\dot{X}\}$ represents the velocity of the vehicle; $\{X\}$ represents the

displacement vector of the vehicle. Since the free vibration can be treated as a superposition of many simple harmonic vibratory motions, the chi-square equation can be obtained as shown in Equation (2).

$$([K] - \omega^2[M])\{\phi\} = 0 \tag{2}$$

Equation (2), ω denotes the inherent frequency; $\{\phi\}$ which denotes the inherent vibration pattern.

Based on the acoustic wave equation, the matrix form of the fluctuation equation without attenuation, ignoring viscous consumption, and the matrix with attenuated fluctuation equation when considering the presence of acoustic damping at the boundary can be derived, as shown in Equations (3) and (4).

$$\left[M_e^P\right]\{\ddot{P}_e\} + \left[K_e^P\right]\{P_e\} + \rho_0\{R_e\}^T\{\ddot{X}_e\} = \{0\} \tag{3}$$

Equation (3), $\lfloor M_e^P \rfloor$ represents the unit fluid mass matrix; $\{P_e\}$ represents the nodal pressure vector; $\lfloor K_e^P \rfloor$ represents the unit fluid stiffness matrix; $\rho_0\{R_e\}^T$ represents the unit coupling mass matrix; and $\{\ddot{X}_e\}$ represents the nodal displacement component vector.

$$\begin{aligned} &\left[M_e^P\right]\{\ddot{P}_e\} + \left[C_e^P\right]\{\dot{P}_e\} + \\ &\left[K_e^P\right]\{P_e\} + \rho_0\{R_e\}^T\{\ddot{X}_e\} = \{0\} \end{aligned} \tag{4}$$

Equation (4), $\lfloor C_e^P \rfloor$ represents the unit fluid damping matrix. In the case of a car using a hard surface with no sound-absorbing material at the boundary, the characteristic equation is calculated as shown in Equation (5).

$$\left[\left[K_e^P\right] - \omega^2\left[M_e^P\right]\right]\{P_e\} = 0 \tag{5}$$

When a car is used with a hard surface bounded by sound-absorbing material, the characteristic equation is calculated as shown in Equation (6).

$$\left[\left[K_e^P\right] + j\omega\left[C_e^P\right] - \omega^2\left[M_e^P\right]\right]\{P_e\} = 0 \tag{6}$$

Equation (6), j represents a constant. Using numerical analysis, the acoustic resonance frequencies and the corresponding sound pressure distributions within the new energy vehicle can be obtained using Equations (5) and (6) for different boundary conditions. To obtain the inherent acoustic mode of the cavity itself, the cavity wall plate must be assumed to be rigid to analyze the acoustic modalities of the noise inside the vehicle using the above research. To describe the acoustic mode shape visually, the concepts of "longitudinal", "transverse", "vertical" and "toroidal" are used. The first 8 orders of acoustic inherent frequencies and mode shapes are described as shown in Table 1.

Table 1. Frequency and vibration patterns of the acoustic modes

Order	Natural frequency/Hz	Vibration mode description
1	36.04	Vertical first order
2	71.56	Vertical second order
3	75.01	Horizontal first order
4	81.96	Vertical first order and horizontal first order
5	99.91	Vertical second-order and horizontal first-order
6	108.05	Vertical third order
7	111.97	Vertical first order
8	124.03	Vertical first order and vertical first order

As can be seen from Table 1, the acoustic pressure pattern of the first-order mode varies mainly along the longitudinal direction, with very little variation in the other directions. The second-order acoustic mode shape also varies along the longitudinal direction, with two nodal surfaces of very small acoustic pressure appearing above the longitudinal cross-section, hence the term longitudinal second-order acoustic mode. The third-order acoustic mode varies mainly along the transverse direction, with a nodal plane of near zero sound pressure in the middle of the transverse section, and is referred to as the transverse first-order acoustic mode. The fourth-order acoustic mode varies mainly along the longitudinal and transverse directions, with an acoustic pressure nodal plane appearing in both the transverse and longitudinal sections, and is therefore referred to as the longitudinal first-order and transverse first-order modes. The fifth-order acoustic mode has two nodal surfaces in the longitudinal section and one nodal surface in the transverse section at the same time and is referred to as the second and transverse first-order acoustic mode.

The sixth-order acoustic mode appears with three nodal planes in the longitudinal direction and is therefore referred to as the longitudinal third-order acoustic mode. The seventh-order acoustic mode has one nodal plane with zero sound pressure in the vertical section and is therefore referred to as the vertical first-order acoustic mode. The sound pressure vibration mode of the eighth-order acoustic mode has two nodes in the longitudinal section and a node with zero sound pressure in the vertical section. In the longitudinal section, the maximum sound pressure value appears at the front top and back top of the cavity, and this mode has the lowest resonance frequency in the longitudinal direction. On the vertical section, the vertical first mode has a nodal plane where the sound pressure is zero, that is, the sound pressure changes the most at this position. This mode has the lowest resonance frequency in the vertical direction, so it is called the longitudinal first order and the vertical first order. The existence of vertical first-order mode and vertical first-order mode is due to the limitation of space structure and boundary conditions, which makes the sound waveform a specific node and anti-node distribution in a specific direction. The presence of this vibration state is important for acoustic design and control and can provide reference and guidance when designing acoustic systems or reducing noise. In addition, the study of vertical and vertical modes is also helpful to understand the propagation law of sound waves in space, to better understand acoustic phenomena and applications.

3.2 Noise Control Technology for New Energy Vehicles based on Acoustic-solid Coupling Theory

During the driving process of a new energy vehicle, the vibration of the body panels by external excitation will produce a kind of pressure on the air around the body panels inside the vehicle, thus changing the sound pressure inside the vehicle, and the change of the sound pressure inside the vehicle will more or less amplify or suppress the vibration of the body panels. This interaction between the structure and the air forms an acoustic-solid coupling system. The new energy vehicle is in fluid during travel and is subjected to fluid pressure, so the vibration equation for a vehicle structure that considers the loading effect of fluid pressure is shown in Equation (7).

$$[M_e]\{\ddot{X}_e\} + [C_e]\{\dot{X}_e\} + [K_e]\{X_e\} = \{F_e\} + \{F_e^{pr}\} \qquad (7)$$

Equation (7), $\{F_e^{pr}\}$ represents the fluid pressure load vector, which is calculated as shown in Equation (8).

$$\{F_e^{pr}\} = \int_S \{N'\}P\{n\}\,dS \qquad (8)$$

Equation (8), S denotes the interface area; $\{N'\}$ denotes the displacement unit shape function; $\{n\}$ and denotes the unit normal of the interface. Substituting the finite unit form function for the spatial variation of pressure into Equation (8), the structural vibration finite element equation for the interface pressure vector can be derived as shown in Equation (9).

$$[M_e]\{\ddot{X}_e\} + [C_e]\{\dot{X}_e\} + [K_e]\{X_e\} - \{R_e\}\{P_e\} = \{F_e\} \quad (9)$$

Equation (9), $\{R_e\}$ denotes the coupling mass matrix. This leads to the finite element matrix equation for the fluid-structure coupling problem, as shown in Eq. (10).

$$\begin{bmatrix} [M_e] & [0] \\ [M^{fs}] & [M_e^P] \end{bmatrix}\begin{Bmatrix} \ddot{X}_e \\ \ddot{P}_e \end{Bmatrix} + \begin{bmatrix} [C_e] & [0] \\ [0] & [C_e^P] \end{bmatrix}\begin{Bmatrix} \dot{X}_e \\ \dot{P}_e \end{Bmatrix} + \begin{bmatrix} [K_e] & [K^{fs}] \\ [0] & [K_e^P] \end{bmatrix}\begin{Bmatrix} X_e \\ P_e \end{Bmatrix} = \begin{Bmatrix} \{F_e\} \\ \{0\} \end{Bmatrix} \qquad (10)$$

Equation (10), $[M^{fs}]$ denotes the cell coupling mass matrix; $[K^{fs}]$ denotes the matrix with negative signs for all elements in the coupling matrix. The finite element analysis results of the internal sound field of a vehicle will be influenced by the finite element model of the vehicle body and its internal cavity, and the accuracy of the finite element model of the vehicle body will also be reflected in the finite element analysis results. Therefore, when building the finite element model of the car body, the model needs to be simplified to make the computer simulation model as close as possible to the actual model of the car. Therefore, the body model is simplified and key points are positioned to create the body model. As each unit node has six degrees of freedom in each direction, i.e. three degrees of freedom for translation in the z-axis, y-axis, and z-axis and three degrees of freedom for rotation around the axis, the type of unit structure designed for the study is shown in Figure 3, [20].
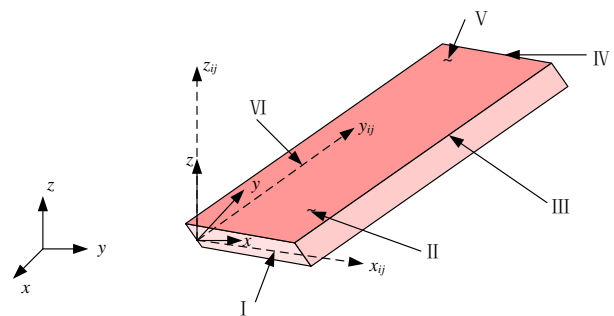
Fig. 3: Cell structure diagram of the degrees of freedom

As can be seen from Figure 3, when the fluid unit is located on the contact surface of the acoustic-solid coupling in the interior cavity of the vehicle, the unit node has four degrees of freedom, including the x-axis, y-axis, and z-axis translational

degrees of freedom, and the acoustic pressure degrees of freedom of the sound field. When the fluid unit is not located on the contact surface of the air-solid in the interior cavity of the vehicle, it has only one degree of freedom, the sound pressure degree of freedom. The calculation of the weight integral of the acoustic-solid coupling in the sound field is shown in Equation (11).

$$\int_V \tilde{p}(\nabla^2 p(x,y,z) - k^2 p(x,y,z) + j\rho_0\omega q(x,y,z))dV = 0$$
(11)

Equation (11), $\tilde{p}$ represents the weight coefficient; ∇^2 represents the Lagrangian operator; $p(x,y,z)$ represents the sound pressure function p in the coordinate system; k and q both represent constants; and ρ_0 represents density. The mathematical expression for the wavelet amplitude in the confined compartment at this point is shown in Equation (12).

$$\nabla^2 \rho_0 = \frac{1}{C_0^2}\frac{\partial p(x,y,z)}{\partial t^2}$$
(12)

Equation (12), C_0 represents the speed of propagation of the acoustic wave; t represents the time; ∂ represents the partial derivative. The equation for the acoustic material state is shown in Equation (13).

$$p' = \frac{\gamma p_0}{\rho_0}\cdot\rho' + \frac{\gamma(\gamma-1)}{2\rho_0^2}\cdot(\rho')^2 + ...$$
(13)

Equation (13), γ represents the ratio of the constant pressure specific heat capacity to the heat capacity of the gas; ρ' represents the density of the fluid; and p' represents the acoustic pressure of the fluid. The kinetic equation on the coordinate axis is shown in Equation (14).

$$\begin{cases} (\rho_0 + \rho')(\frac{\partial}{\partial t} + v\Box\nabla)v_x = \frac{\partial(p_0 + p')}{\partial x} \\ (\rho_0 + \rho')(\frac{\partial}{\partial t} + v\Box\nabla)v_y = \frac{\partial(p_0 + p')}{\partial y} \\ (\rho_0 + \rho')(\frac{\partial}{\partial t} + v\Box\nabla)v_z = \frac{\partial(p_0 + p')}{\partial z} \end{cases}$$
(14)

Equation (14), p_0 represents the sound pressure at rest; v_x, v_y and v_z represents the velocity in the x, y, and z directions respectively; ∇ represents the velocity change value. Equation (14) is combined with the vector to obtain Equation (15).

$$(\rho_0 + \rho')(\frac{\partial}{\partial t} + v\Box\nabla)v = -\nabla(p_0 + p')$$
(15)

The workflow for the finite element analysis of the acoustic-solid coupling of the noise inside the vehicle is therefore shown in Figure 4.
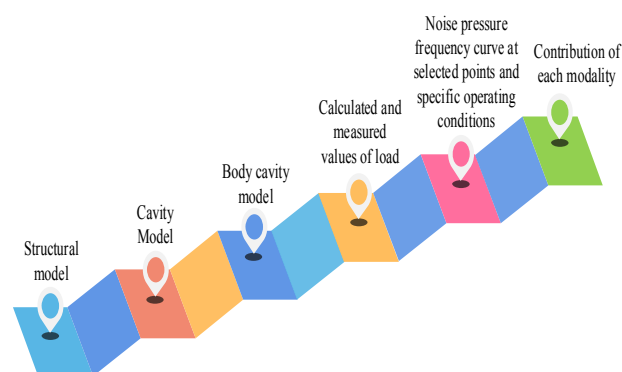
Fig. 4: Flow chart of acoustic-solid coupling analysis

As can be seen from Figure 4, the air finite element model of the internal cavity of the car and the structure of the car itself, as well as the solid-fluid coupling model of the mutual coupling between the two, are first established. Then the finite element simulation of the acoustic-solid coupling is established and the response of the sound field, sound pressure distribution, and excitation points under a specific load condition are calculated by the finite element simulation. The response of the interior cavity structure of the vehicle is obtained for each order of the modal sound field and the contribution of the corresponding structural body members to this response. The finite element model of the acousto-solid coupled system is shown in Figure 5.
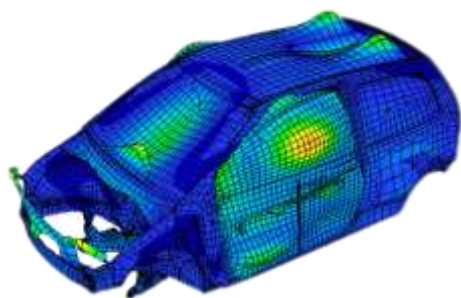
Fig. 5: Acoustic-solid coupling system model

As shown in Figure 5, since the coupled mode is formed by the interaction between the body structure and the air, the coupled mode vibration distribution is partly dominated by the structural deformation and partly by the sound pressure variation, which corresponds to the two systematic modes of the structure and the acoustic cavity respectively. In summary, this paper proposes to use the sound-structure coupling theory and the structural modal analysis of new energy vehicles to build a sound-structure coupling system model for accurate monitoring of vehicle noise. Firstly, the finite element model of the new energy body structure is established, the modal natural frequency and vibration mode of the body structure are calculated, and the vibration components are found through the structural modes. Then, the acoustic finite element model of the interior cavity and the acoustic-solid coupling model are established, the acoustic natural mode and frequency are calculated, and the sound pressure deformation is the main mode and frequency under the coupling action, to realize the accurate monitoring of the interior noise of new energy vehicles.

4 Analysis of the Application Effect of Noise Control Technology of New Energy Vehicles Combined with Sound-solid Coupling

To analyze the effect of the practical application of the research-proposed noise control technology for new energy vehicles optimized using acoustic-solid coupling theory, the research will use real vehicle road tests. A new energy vehicle of a certain brand will be used as the test vehicle, in which acceleration sensors, microphones, and data collectors will be installed, and a computer will be connected to conduct the test using LMS software. The study will take the frequency response of the new energy vehicle body vibration and the sound pressure frequency response inside the vehicle as the main test objects of this test.

4.1 New Energy Vehicle Body Vibration Frequency Response Analysis

To analyze the frequency response of the new energy vehicle body vibration, test points were set up on the roof and floor of the test vehicle respectively, and the change in vibration acceleration at the test points was recorded through a series of external excitation signals, and the test results are shown in Figure 6.

(a) Roof panel test point

(b) Underbody test point
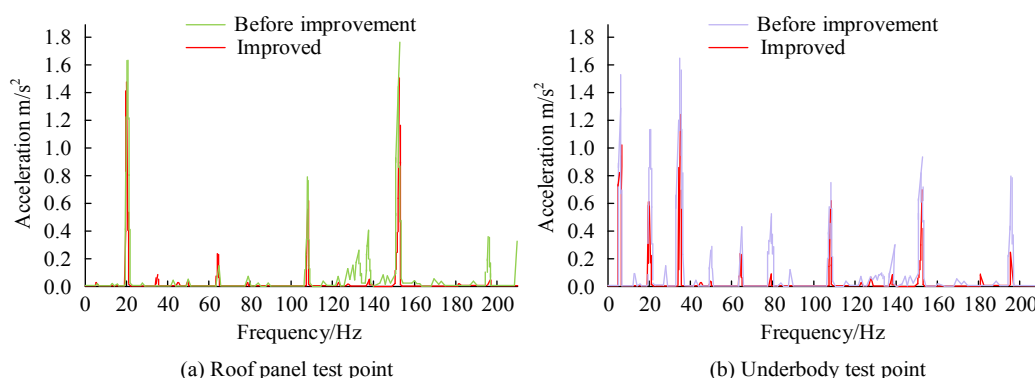
Fig. 6: Vibration acceleration of the test point of automobile roof and bottom plate

(a) Before improvement   (b) After improvement
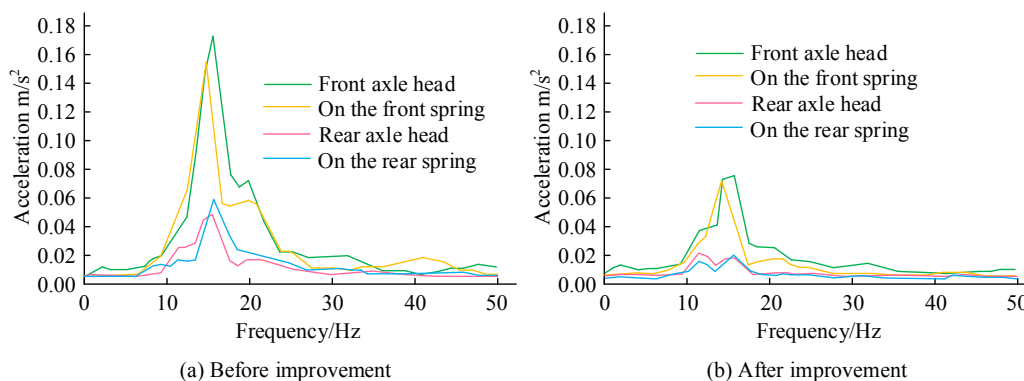
Fig. 7: The vibration spectrum on the front and rear axle head and spring of the car

Table 2. The vibration frequency of the automobile engine at different speeds

	Driving speed (km/h)	30	60	80
	Engine speed (rpm)	1000	1300	1500
Before the improvement	Excited frequency (Hz)	60	75	79
	Vibration frequency of suspension rack (Hz)	50	62	73
After the improvement	Excited frequency (Hz)	50	60	70
	Vibration frequency of suspension rack (Hz)	43	50	62

From Figure 6(a), it can be seen that at the external excitation frequency range of 0-200 Hz, the vibration of the test point of the car roof is obvious at about 20 Hz, 108 Hz, and 150 Hz. The acceleration of the test point before the improved noise control technology is 1.61 m/s², 0.89 m/s² and 1.71 m/s² respectively. The acceleration of the test point after the improved noise control technology is 1.48 m/s², 0.61 m/s², and 1.43 m/s² respectively. From Figure 6(b), it can be seen that when the external excitation frequency is in the range of 0-200 Hz, the vibration of the test point of the car floor is obvious at 5 Hz, 35 Hz, 50 Hz, 105 Hz, 153 Hz, and 195 Hz. After the improvement of noise control technology, the acceleration of the test points were 1.02 m/s², 0.59 m/s², 0.62 m/s², 0.67 m/s², 0.71 m/s², 0.33 m/s². The test points were set up at the front axle head, the front spring, the rear axle head, and the rear spring, and the changes in

vibration acceleration at the test points were recorded while the car was traveling at a speed of 50 km/h. The test results are shown in Figure 7.

As can be seen from Figure 7, the external excitation frequency range generated during the car's uniform speed is 0-50 Hz, with all test points producing peak vibration at a frequency of around 15 Hz. The peak vibration accelerations at the front axle head, on the front spring, on the rear axle head, and the rear spring were 0.175 m/s², 0.158 m/s², 0.043 m/s², and 0.059 m/s² respectively, when the vehicle was not using the improved noise control technology. After improvement, the peak vibration accelerations were 0.080 m/s², 0.078 m/s², 0.020 m/s², and 0.019 m/s² respectively. The excitation frequencies of the car and the suspension vibration frequencies were recorded when the car was driven forward at different driving speeds. The test results are shown in Table 2.

As can be seen from Table 2, when the speed of the car is 30 km/h, the speed of the car engine is 1000 rpm, before using the improved noise control technology, its excitation frequency is 60 Hz and the vibration frequency of the suspension is 50 Hz; after using the improved noise control technology, its excitation frequency is 50 Hz and the vibration frequency of the suspension is 43 Hz. when the speed of the car is 60 km/h, the speed of the car engine is 1300 rpm, before using the improved noise control technology, its excitation frequency is 75 Hz and the vibration frequency of the suspension is 62 Hz. At a speed of 60 km/h, the

engine of the car rotates at 1300 rpm, before using the improved noise control technology, the excitation frequency is 75 Hz and the vibration frequency of the suspension is 62 Hz; after using the improved noise control technology, the excitation frequency is 60 Hz and the vibration frequency of the suspension is 50 Hz. The excitation frequency is 79 Hz and the suspension vibration frequency is 73 Hz; after using the improved noise control technology, the excitation frequency is 70 Hz and the suspension vibration frequency is 62 Hz. The frequency response analysis of body vibration refers to the analysis of the vibration generated by the vehicle during operation to determine the main frequency and amplitude of the vibration, understand the vibration intensity of the vehicle under different frequencies, determine the structural strength and comfort level of the vehicle, and detect the fault or abnormal situation of the vehicle. In the field of automotive engineering, the analysis of body vibration frequency response is an important research direction, that is of great significance in improving the performance and safety of vehicles. Through the comparison of the vibration acceleration changes of the test points of the roof and side panels of new energy vehicles, the results show that the vibration acceleration of the test points has decreased after improving the noise control technology. By comparing the vibration acceleration peaks of the test points of the front axle head, front spring, rear axle head, and rear spring of new energy vehicles, the results show that the vibration acceleration peaks of the test points after the improvement of noise control technology are all lower than the peak before the improvement. By recording the exciting frequency and suspension vibration frequency of new energy vehicles at different driving speeds, the results show that the exciting frequency and suspension vibration frequency of new energy vehicles are reduced after the improvement of noise control technology. The above results show that the technology can reduce vibration intensity, reduce noise, and improve comfort.

4.2 Frequency Response Analysis of Sound Pressure in New Energy Vehicles

To analyze the sound pressure frequency response inside the new energy vehicle, the study set up test points at the windscreen and side window glass of the vehicle, and recorded the noise pressure value at the test points under the change of engine speed, the test results are shown in Figure 8.

From Figure 8(a), it can be seen that at the test point at the windscreen of the car, the noise pressure value reaches the highest when the engine speed reaches 3500 r/min, and the noise pressure values before and after using the improved noise control technology are 93 dB(A) and 80 dB(A) respectively, and the noise pressure values after using the improved noise control technology are lower than before the improvement. As can be seen from Figure 8(b), before the use of the improved noise control technology, the test point at the side window glass of the car reached a maximum noise pressure value of 90 dB(A) when the engine speed reached 3500 r/min. After the use of the improved noise control technology, the test point at the side glass of the car reached a maximum noise pressure of 73 dB(A) at an engine speed of 2000 r/min. The noise pressure values after the improved noise control technology were lower than before the improvement. The sound pressure at the ear of the driver, co-driver, and rear passenger was measured and recorded at different operating conditions and the test results are shown in Table 3.

(a) Change in sound pressure at the windshield

(b) Change in sound pressure at the side window glass
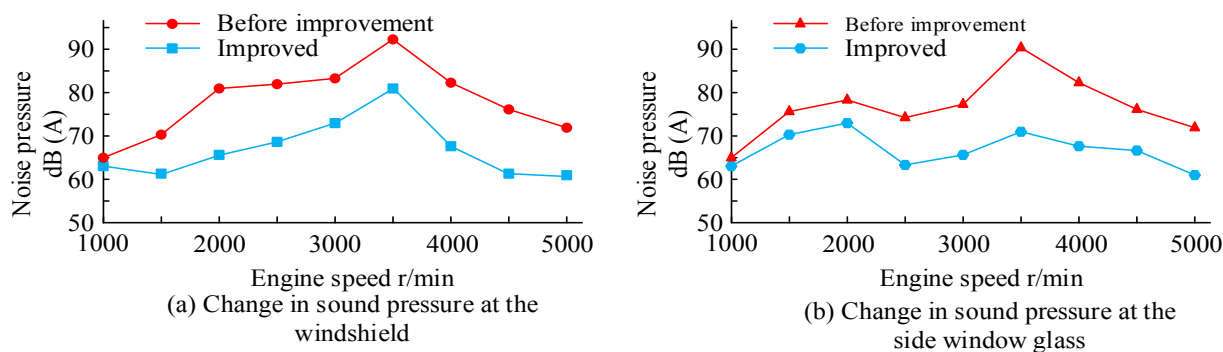
Fig. 8: Noise value at the automotive glass

Table 3. Sound pressure value in cars

Working condition (rpm)	Driver sound pressure/dB(A)		Co-pilot sound pressure/dB(A)		Rear personnel sound pressure/dB(A)	
	Before	After	Before	After	Before	After
800	78	74	80	77	76	71
1400	74	72	76	73	72	70
2500	85	81	80	77	81	79

As can be seen from Table 3, the sound pressure at the driver's, co-driver, and rear passenger's ears was 78 dB(A), 80 dB(A), and 76 dB(A) respectively before the use of the improved noise control technology at 800 rpm. With the improved noise control technology, the sound pressure at the driver's, co-drivers, and rear passenger's ears is 74 dB(A), 77 dB(A), and 71 dB(A) respectively. At 1400 rpm, the sound pressure at the driver's, co-

drivers, and rear passenger's ears was 74 dB(A), 76 dB(A), and 72 dB(A) respectively before the use of the improved noise control technology. With the improved noise control technology, the sound pressure at the driver's, co-drivers, and rear passenger's ears is 72 dB(A), 73 dB(A), and 70 dB(A) respectively. At 2500 rpm, the sound pressure at the driver's, co-driver's and rear passenger's ears were 85 dB(A), 80 dB(A), and 81 dB(A) respectively before the use of the improved noise control technology. With the improved noise control technology, the sound pressure at the driver's, co-drivers, and rear passenger's ears was 81 dB(A), 77 dB(A), and 79 dB(A) respectively. The sound pressure at the driver's side of the ear in the car was recorded while the car was driven at 50 km/h on a concrete and asphalt road and the results are shown in Figure 9.

(a) Cement pavement

(b) Asphalt pavement
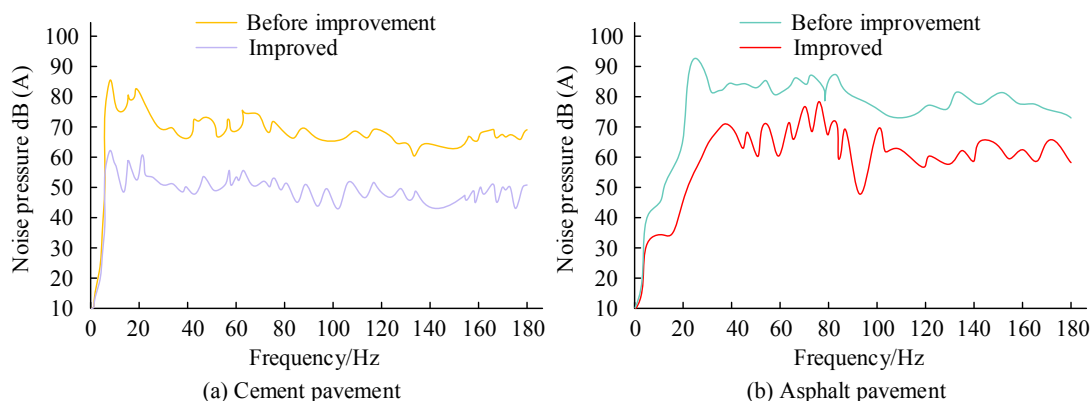
Fig. 9: Sound pressure value curve of vehicles on different road surfaces

Table 4. Simulation error of the finite element model for improved noise control techniques

Serial number	Error type	35 Hz	70 Hz	100 Hz
1	Model assumption error	1.00%	1.04%	0.09%
2	Calculation method error	1.01%	1.01%	1.00%
3	Calculation accuracy error	0.09%	1.00%	1.03%

Figure 9(a) shows that when the car is driven on concrete roads, the maximum sound pressure next to the driver's ear is 62 dB(A) after using the improved noise control technology, which is lower than 86 dB(A) before using the technology. Figure 9(b) shows that when the vehicle is driven on asphalt, the maximum sound pressure next to the driver's ear is 77 dB(A) after using the improved noise control technology, which is lower than the 92 dB(A) before using the improved noise control technology. The frequency response analysis of the sound pressure inside the car refers to the frequency response analysis of the noise inside the car to understand the amplitude and characteristics of the noise inside the car at different frequencies. In-vehicle sound pressure frequency response analysis can also help detect vehicle noise problems, identify noise sources, and find solutions. Test points were set at the windscreen and side window of new energy vehicles to record the noise pressure value at the test point. The test results show that the noise pressure value after using the improved noise control technology is lower than before. By detecting and recording the sound pressure near the ear of the driver, co-driver, and rear passenger of the new energy vehicle, we can see by comparing the structure that under different vehicle working conditions, the sound pressure near the ear of the driver, co-driver and rear passenger is reduced after using the improved noise control technology. The results show that the maximum and minimum of the sound pressure near the driver's ear are reduced by using the improved noise control technology. Combining all the above test results, the improved noise control technique is feasible. To further explore the performance of the improved noise control technology, the simulation error analysis of the finite element model is studied, and the test results are shown in Table 4.

As can be seen from Table 4, in the simulation error analysis of the finite element model of the improved noise control technology, it is found that when the internal noise frequency of new energy vehicles is 35 Hz, 70 Hz, and 100 Hz, the model hypothesis error, calculation method error, and calculation accuracy error of the improved noise control technology are all floating around 1.00%, which is a small error. The result further verifies the superiority of the improved noise control technology.

At present, the commonly used internal noise control technologies include acoustic isolation technology, shock absorbers, active noise control technology, engine sound insulation, aerodynamic optimization technology, and so on. Acoustic isolation technology can effectively isolate the transmission and radiation of noise and provide a good driving environment. However, this technology increases the weight and cost of the vehicle, which can affect the fuel economy of the vehicle. The installation of damping devices can effectively reduce the vibration and noise caused by road noise and bumps, and improve driving comfort. However, it increases the cost of the vehicle and puts forward higher requirements for the design and maintenance of the suspension system. Active noise control technology uses sensors and control systems to control reverse sound waves to counteract noise. This technology can create offset sound waves inside the car, reducing noise levels. The advantage is that it can provide a better noise control effect, which is not limited by the structure and material of the vehicle. However, the technology requires complex sensors and control systems, adding complexity and cost to the vehicle. Engine soundproofing can effectively reduce the conduction and radiation of engine noise, providing a quieter driving experience. However, it will have a certain impact on the heat dissipation of the engine. Aerodynamic optimization technology reduces noise caused by wind noise and wind resistance by optimizing the body and parts design but affects the exterior design and performance of the vehicle. The noise control technology of new energy vehicles proposed in this study is based on the vehicle structure of finished vehicles, and the acoustic-solid coupling theory is proposed to carry out modal analysis of new energy vehicle structure, optimize the noise control technology of new energy vehicles, and build an acoustic-solid coupling system model to accurately monitor the internal noise of vehicles. This method can effectively control the noise in the driving process of new energy vehicles, reduce the negative impact of noise, and does not increase the cost of vehicle design and research and development, which is better than the commonly used internal vehicle noise control technology.

5 Conclusion

With the continuous development of automotive technology, the performance of cars is gradually improved, and due to the influence of the concept of sustainable development, people's requirements for cars, in addition to meeting the basic conditions of safety performance, also require its low-carbon environmental protection. Therefore, the emergence of new energy vehicles has attracted much attention, but the noise generated by these vehicles during the driving process is large and affects the comfort of the occupants and the concentration of the driver. The study therefore proposes to improve the noise control technology of new energy vehicles using acoustic-solid coupling theory. The results show that the maximum vibration acceleration at the top plate, bottom plate, axle head, and spring of the vehicle are 1.48 m/s^2, 1.02 m/s^2, 0.079 m/s^2, and 0.020 m/s^2 respectively, which are lower than the maximum vibration acceleration before the use of the technology. The vibration frequencies of the suspension after the use of this technology were 43 Hz, 50 Hz, and 62 Hz respectively at different speeds of the car, all lower than before the use. The maximum noise pressure values detected at the windscreen and side window glass were 80 dB(A) and 73 dB(A) respectively after the use of this technology. The sound pressure at the driver's, passenger's, and rear passenger's ears at 800 rpm was 74 dB(A), 77 dB(A) and 71 dB(A) respectively, all lower than before. The maximum sound pressure at the driver's ear after using the improved technology is 62 dB(A) and 77 dB(A) respectively when the car is driven on different roads, which are lower than before. In summary, the study proposes to improve the noise control technology of new energy vehicles by combining sound-solid coupling theory, which can effectively reduce the noise generated by new energy vehicles and improve the comfort of vehicle occupants. However, in the process of research, the pores in the carriage of new energy vehicles and the vibration of the body skin, as well as the weight of the engine, clutch, and other transmission systems and the air conditioning in the car are ignored. It is hoped that we can pay more attention to the leakage noise, strengthen the modeling accuracy, and improve the credibility of the simulation. At the same time, interior materials such as seats, instrument panel assembly, and carpet make the distribution of the interior sound field more complicated, which has not been explored in this study. It is hoped that the sound-absorbing characteristics of interior materials can be corrected by testing in the future, and the influence of interior materials on the interior sound field can be analyzed in detail.

References
[1] D. Ma, N.S hlezinger, T. Huang, Y. Liu, and Y. Eldar, Joint Radar-communication Strategies for Autonomous Vehicles: Combining Two Key Automotive Technologies, *IEEE Signal Processing Magazine*, vol.37 no.4, 2020, pp.85-97.

[2] M. Moslehpour, K. Chau, Y. Tu, L. Khanh, B. Momodou, D. Kamasani, Impact of Corporate Sustainable Practices, Government Initiative, Technology Usage, and Organizational Culture on Automobile Industry Sustainable Performance, *Environmental Science and Pollution Research*, vol.29, no.55, 2022, pp.83907-83920.

[3] D. Pathak, A. Verma, V. Kumar, Performance Variables of GSCM for Sustainability in Indian Automobile Organizations Using TOPSIS Method, *Business Strategy & Development*, vol.3, no.4, 2020, pp.590-602.

[4] X. Tian, Q. Zhang, Y. Chi, Y. Cheng, Purchase Willingness of New Energy Vehicles: A Case Study in Jinan City of China, *Regional Sustainability*, vol.2, no.1, 2021, pp.12-22.

[5] X. Li, X. Xiao, H. Guo, A Novel Grey Bass Extended Model Considering Price Factors for the Demand Forecasting of European New Energy Vehicles, *Neural Computing and Applications*, vol.34, no.14, 2022, pp.11521-11537.

[6] J. Kim, S. Cho. Deep CNN Transferred from VAE and GAN for Classifying Irritating Noise in Automobile, *Neurocomputing*, vol.452, no.10, 2021, pp.395-403.

[7] W. Yu, Z. Huang, C. Zhong, J. Liu, Z. Yuan, Method of Suppressing Torsional Vibration Noise of Automobile Drive-train System Based on Discrete Wavelet, *Journal of Intelligent & Fuzzy Systems*, vol.38, no.6, 2020, pp.7585-7594.

[8] S. Wang, X. Yu, L. Shen, A. Yang, E. Chen, J. Fieldhouse, D. Barton, S. Kosarieh, Noise Reduction of Automobile Cooling Fan Based on Bio-inspired Design, *Proceedings of the Institution of Mechanical Engineers, Part D: Journal of Automobile Engineering*, vol.235, no.2-3, 2021, pp.465-478.

[9] Y. He, S. Wen, Y. Liu, Z. Yang, Wind Noise Source Characterization and Transmission

Study through a Side Glass of DrivAer Model Based on a Hybrid DES/APE Method, *Proceedings of the Institution of Mechanical Engineers, Part D: Journal of Automobile Engineering*, vol.235, no.6, 2021, pp.1757-1766.

[10] K. Chen, X. Zhang, Y. Liu, J. Ma, An Improved Denoise Method Based on EEMD and Optimal Wavelet Threshold for Model Building of OPAX, *Proceedings of the Institution of Mechanical Engineers, Part D: Journal of Automobile Engineering,* vol.235, no.14, 2021, pp.3530-3544.

[11] C. Gan, Y. Chen, X. Cui, J. Sun, R. Qu, J. Si, Comprehensive investIgation of Loss Calculation and Sequential Iterative Fluid-solid Coupling Schemes for High-speed Switched Reluctance Motors, *IEEE Transactions on Energy Conversion*, vol.36, no.2, 2021, pp.671-681.

[12] H. Hou, T. Rui, R. Deng, Z. Xu, S. Liu, Modal Analysis of Central Impression Cylinder Based on Fluid-solid Coupling Method, *Journal of Low Frequency Noise Vibration and Active Control*, vol.40, no.2, 2020, pp.772-783.

[13] L. Li, D. Tan, Z. Yin, T. Wang, X. Fan, R. Wang, Investigation on the Multiphase Vortex and Its Fluid-solid Vibration Characters for Sustainability, *Renewable Energy*, vol.175, no.9, 2021, pp.887-909.

[14] A. Franci, Lagrangian Finite Element Method with Nodal Integration for Fluid-solid Interaction, *Computational Particle Mechanics*, vol.8, no.2, 2021, pp.389-405.

[15] X. Wang, Z. Jin, J. Liu, 2.04 μm Harmonic Noise-like Pulses Generation from a Mode-locked Fiber Laser Based on Nonlinear Polarization Rotation, *Optoelectronics Letters*, vol.17, no.1, 2021, pp.18-21.

[16] A. Stroescu, M. Cherniakov, M. Gashinova, Classification of High Resolution Automotive Radar Imagery for Autonomous Driving Based on Deep Neural Networks, *2019 20th International Radar Symposium (IRS)*, (Ulm, Germany), pp. 1-10, 26-28 June 2019.

[17] M. Dolan, K. Jorabchi, Effects of Outdoor Weathering and Laundering on the Detection and Classification of Fluorinated Oil- and Water-repellent Fabric Coatings, *Journal of Forensic Sciences*, vol.66, no.5, 2021, pp.1669-1678.

[18] S. Fialko, V. Karpilovskyi, Block Subspace Projection Preconditioned Conjugate Gradient Method in Modal Structural Analysis, *Computers & Mathematics with Applications*, vol.79, no.12, 2022, pp.3410-3428.

[19] S. Debnath, Fuzzy Quadripartitioned Neutrosophic Soft Matrix Theory and Its Decision-making Approach, *Journal of Computational and Cognitive Engineering*, vol.1, no.2, 2022, pp.88-93.

[20] I. Shugurov, S. Zakharov, S. Ilic, Dpodv2: Dense Correspondence-based 6 dof Pose Estimation, *IEEE Transactions on Pattern Analysis and Machine Intelligence*, vol.44, no.11, 2021, pp.7417-7435.

Contribution of Individual Authors to the Creation of a Scientific Article (Ghostwriting Policy)

The author FUJUN MAO contributed to the present research, at all stages from the formulation of the problem to the final findings and solution.

Sources of Funding for Research Presented in a Scientific Article or Scientific Article Itself

Conflict of Interest

The author has no conflicts of interest to declare that are relevant to the content of this article.

Creative Commons Attribution License 4.0 (Attribution 4.0 International, CC BY 4.0)